

NUMERICAL SCHEMES FOR ADVANCED REFLECTANCE MODELS FOR SHAPE FROM SHADING

Oliver Vogel

Faculty of Mathematics and Computer Science
Saarland University, Campus E1.1
66041 Saarbrücken
Germany

Emiliano Cristiani

Department of Mathematics
SAPIENZA – Università di Roma
00185 Rome
Italy

ABSTRACT

In recent years, Shape from Shading (SfS) research has been dominated by the rise of perspective models and advanced numerical schemes, which allowed for impressive results compared to previous methods in the field. Despite of these groundbreaking developments, researchers concentrated on Lambertian reflectance models. Recently, some researchers started to include more advanced reflectance models into the Lambertian state-of-the-art model of Prados and Faugeras. Such methods include simple models for specular reflectance, which is of particular importance when reconstructing shiny objects. Other models replace Lambertian reflectance by more advanced types of diffuse reflectance like the Oren-Nayar model, which is of particular importance for the reconstruction of human skin. We review these reflectance models and discuss their compatibility with the state-of-the-art numerical solvers for SfS, both iterative and non-iterative.

Index Terms— Shape from Shading, Numerical Methods

1. INTRODUCTION

Shape from Shading (SfS) is the problem of determining the three-dimensional shape of objects from the brightness information contained in a single two-dimensional image. In recent years, research on SfS has drastically changed. Prados et al. [1] proposed a novel partial differential equation (PDE) to be associated to the problem, as well as a numerical method to solve this PDE. In this model, very different assumptions to classic SfS models have been used, such as perspective projection and a point light source in the optical centre of the projection. In addition, they model the inverse-square law for the attenuation of the light source. This allowed for a nearly well-posed model [2] and results of impressive quality which have not been achievable with classic methods.

However, as in most classic works on SfS, the model is based on Lambertian reflectance. The use of two more advanced reflectance models has been proposed, which allow

to apply SfS to a larger class of images. One is the Phong reflectance model [3], which extends the Lambertian model by specular highlights. A second model is the Oren-Nayar model [4], which replaces Lambertian reflectance by a more realistic model, particularly well-suited for rough surfaces.

Our Contribution. We briefly review these two non-Lambertian reflectance models for SfS. We discuss different options for numerical schemes to solve the underlying PDEs and their computational performance. We propose an efficient iterative scheme which is applicable to both models and present a way to derive a suitable stability limit to the (fictitious) time step which has to be introduced, and can even be chosen adaptively over the image. By means of a numerical test we will show that the discretisation is compatible with so-called Fast Marching algorithms, which allow for very fast solution of the equations. Finally, we evaluate the performance of the proposed scheme in comparison with a classic one.

2. REFLECTANCE MODELS

Perspective SfS methods are based upon solving so-called Hamilton-Jacobi (HJ) equations, which are hyperbolic PDEs of the form

$$H(\mathbf{x}, u(\mathbf{x}), \nabla u(\mathbf{x})) = 0, \quad \mathbf{x} \in \Omega, \quad (1)$$

where the set $\Omega \subset \mathbb{R}^2$ represents the image's domain. The function H is called *Hamiltonian*. In the following, we review the two existing non-Lambertian models and their corresponding Hamiltonians. The depth of the surface can be easily recovered by solutions of these equations.

2.1. Phong model

The first model we discuss is the Phong model as used for SfS in [3]. Here, the Lambertian model is extended by terms for

ambient and specular reflection. The corresponding underlying brightness equation reads as

$$I = k_a I_a + \sum_{\text{light sources}} \frac{1}{r^2} (k_d I_d \cos \phi + k_s I_s (\cos \theta)^\alpha) \quad (2)$$

where I_a , I_d , and I_s are the intensities of the ambient, diffuse, and specular components of light, respectively. ϕ denotes the angle between light source direction and surface normal. The constants k_a , k_d , and k_s with $k_a + k_d + k_s \leq 1$ denote the ratio of ambient, diffuse, and specular reflection. The amount of specular light reflected towards the viewer is proportional to $(\cos \theta)^\alpha$, where θ is the angle between the ideal mirror reflection direction of the incoming light and the viewer direction, and α is a constant modelling the roughness of the material. Finally, $r = r(\mathbf{x})$ is the distance between the light source and surface points.

In the specific setting of a SfS model with a single light source located at the optical centre, we have $2\phi = \theta$. With this simplifying assumption, we can derive [3] the equation

$$\frac{f^2 W}{Q} (I - k_a I_a) - k_d I_d e^{-2v} - \frac{W k_s I_s e^{-2v}}{Q} R^\alpha = 0 \quad (3)$$

$$\text{with } W := \sqrt{f^2 \|\nabla v(\mathbf{x})\|^2 + (\nabla v(\mathbf{x}) \cdot \mathbf{x})^2 + Q^2} \quad (4)$$

$$Q := f / \left(\sqrt{\|\mathbf{x}\|^2 + f^2} \right) \quad (5)$$

$$R := (2Q^2 / W^2) - 1 \quad (6)$$

where $v = \ln u$ is the logarithm of the sought depth, f is the focal length and $\|\cdot\|$ denotes the Euclidean norm.

2.2. Oren-Nayar model

In the Oren-Nayar reflectance model as used for SfS by Ahmed and Farag [4], a rough surface is stochastically modelled by many small facets, each of which is modelled by Lambertian reflectance. In essence, its underlying brightness equation reads as

$$I = \frac{1}{r^2} \frac{\rho}{\pi} L_i \cos \phi_i (A + B \sin \alpha \tan \beta \max(0, \cos(\phi_r - \phi_i)))$$

where L_i is the intensity of the light source, ρ the albedo of the surface, ϕ_i the angle between surface normal and light source direction, ϕ_r the angle between surface normal and observer direction, $\alpha = \max(\phi_i, \phi_r)$, $\beta = \min(\phi_i, \phi_r)$, $A = 1 - 0.5 \frac{\sigma^2}{\sigma^2 + 0.33}$, $B = 0.45 \frac{\sigma^2}{\sigma^2 + 0.09}$, and σ being the standard deviation of the Gaussian distribution used in modelling the distribution of the facets. Parameter σ can be understood as a measure of the roughness of the surface. In the specific setting of the point light source located in the optical centre, we obtain $\phi := \phi_i = \phi_r = \alpha = \beta$. This greatly simplifies the brightness equation and leads to the equation

$$0 = f^2 I \frac{M + 1}{A \sqrt{M + 1} + BM} - e^{-2v} \quad (7)$$

with

$$M = \left[f^2 \|\nabla v(\mathbf{x})\|^2 + (\nabla v(\mathbf{x}) \cdot \mathbf{x})^2 \right] \left(\frac{\|\mathbf{x}\|^2 + f^2}{f^2} \right). \quad (8)$$

3. NUMERICAL METHODS

Most methods proposed for SfS are iterative. In principle, all these methods follow the same approach. For a given Hamiltonian, the iteration

$$v^{(k+1)} = v^{(k)} - \tau \tilde{H}(\mathbf{x}, v^{(k)}(\mathbf{x}), \tilde{\nabla} v^{(k)}(\mathbf{x})) \quad (9)$$

is performed, starting from some suitable initial guess $v^{(0)}$. \tilde{H} is called the discrete Hamiltonian and $\tilde{\nabla}$ is the discrete gradient. The parameter $\tau > 0$ is a (fictitious) time step introduced to write the equation in a fixed point form.

A general-purpose method of discretising such HJ equation is the Lax-Friedrichs (LF) method [5]. This method is employed by Ahmed and Farag [4] for the Oren-Nayar model. The discrete Hamiltonian of the LF method approximating (1) reads as

$$\begin{aligned} \tilde{H} := & H(\mathbf{x}, v(\mathbf{x}), \tilde{\nabla} v(\mathbf{x})) \\ & + \frac{\alpha_1}{2} \left(\frac{v_{i+1,j} - 2v_{i,j} + v_{i-1,j}}{h} \right) \\ & + \frac{\alpha_2}{2} \left(\frac{v_{i,j+1} - 2v_{i,j} + v_{i,j-1}}{h} \right) \end{aligned} \quad (10)$$

where h is the space discretisation step (in both x_1 and x_2 directions), and

$$\alpha_1 \geq \max_{\Omega} |H_{\frac{\partial v}{\partial x_1}}(\mathbf{x}, v, \nabla v)|, \quad \alpha_2 \geq \max_{\Omega} |H_{\frac{\partial v}{\partial x_2}}(\mathbf{x}, v, \nabla v)|.$$

In practice, we need to compute α_1 and α_2 at the beginning of each iteration. The LF method is generally rather slow and tends to smear out solutions. In addition, it is rather difficult to find a good estimate for the parameter τ .

A much more efficient discretisation of spatial derivatives is the so-called Upwind scheme used in [6]. This is not suitable for all Hamiltonians, in general we can only be sure on convex Hamiltonians w.r.t. ∇v . For SfS, the Lambertian Hamiltonian is convex [1], however for the non-Lambertian case this does not hold. Nevertheless, it is also possible to obtain a stable scheme when applying an Upwind scheme to certain non-convex Hamiltonians.

In an Upwind scheme, spatial derivatives are approximated by one-sided difference approximations in the "right" direction. For the x_1 -derivative of v , we simply determine

$$\min \left\{ \frac{v_{i+1,j} - v_{i,j}}{h}, \frac{v_{i-1,j} - v_{i,j}}{h}, 0 \right\}. \quad (11)$$

If the first or third term of this set is the smallest, we simply take this as the derivative. If the second term is the smallest,

we take this as the derivative after reversing its sign. In x_2 -direction, we proceed analogously as in the x_1 -direction.

Using an Upwind scheme has several advantages over the LF method. There is no need to precompute maxima over derivatives of the Hamiltonian at the beginning of each iteration. This has the consequence that it is possible to use updated values of v during the iteration once available, similar to the Gauss-Seidel method for solving linear systems. This significantly improves the rate of convergence of the method, resulting in a much faster method. Furthermore, Upwind schemes are significantly easier to implement than a LF scheme.

Another advantage of the Upwind method is that it is significantly easier to determine an upper bound for the time step size than for the LF method. In essence, we need to find an upper bound of the discretised version of the Hamiltonian \tilde{H} such that, for some $\tau_0 > 0$, we have

$$\tilde{H} \leq \frac{\delta v}{\tau_0} \quad (12)$$

where δv is the absolute value of the discretised spatial gradient, see [7]. Then, the scheme will be stable for all $\tau < \tau_0$. By a derivation similar to the one done in [7], we can obtain an upper bound for both the Phong as well as the Oren-Nayar Hamiltonian. For the Phong model, we obtain the bound

$$\tau \leq \frac{Q}{(I - k_a I_a) f^2 \sqrt{2f^2 + \alpha \|\mathbf{x}\|^2}} \quad (13)$$

and for the Oren-Nayar model we obtain the bound

$$\tau \leq \frac{Af}{\sqrt{\|\mathbf{x}\|^2 + f^2}(\sqrt{2f + 2\|\mathbf{x}\|})}. \quad (14)$$

Note that it is possible to choose these time steps adaptively for every pixel instead of choosing one common value for the entire image. This results in a further speed-up of the method.

Furthermore, using an Upwind scheme, it is possible to use a Fast Marching algorithm, which has been described for the Phong model in [8]. It is a non-iterative algorithm in which the nodes of the grid are visited in a special order, which is found by the algorithm itself. The same procedure is also possible for the Oren-Nayar model.

4. EXPERIMENTS

In this section, we evaluate the performance of the different numerical methods on a standard example, the Mozart face surface. We used the original version of the image which can be downloaded from the webpage of the authors of [9]. This version contains several peaks and discontinuities, which make the reconstruction particularly difficult. The size of the image is 256×256 pixels and the focal length f is 500 times the pixel size. The first row of Figure 1 shows two different input images, one being a rendered version of the surface

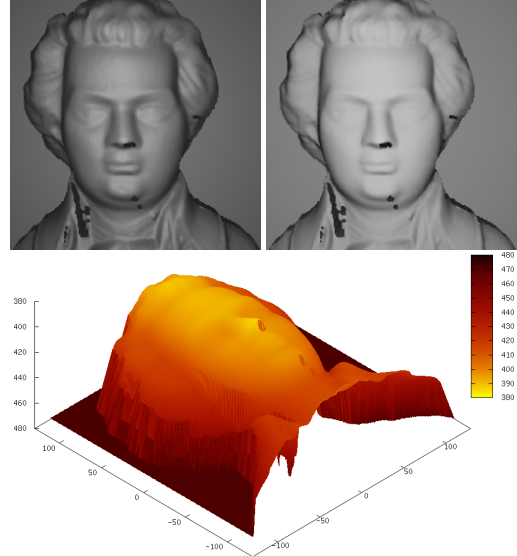


Fig. 1. Shape from Shading on the Mozart face. Top: Input images (Phong, Oren-Nayar). Bottom: Ground truth.

using the Phong model with 20% specular reflectance and $\alpha = 5$, the second using the Oren-Nayar model with $\sigma = 0.5$. The bottom row of Figure 1 shows the ground truth surface for this experiment.

The reconstructed surfaces are displayed in Figure 2. The plots show the reconstructions obtained using an Upwind scheme. Visually, both look convincing, the Hamiltonian modelling the Phong model tends to smear edges while the Oren-Nayar model generally allows for sharper edges, including the peaks in the surface. We did not include plots of the result achieved using the LF discretisation, as the results look very similar, including their behaviour at discontinuities. Initialisation in all cases was an upper bound for the depth in this experiment. Boundary conditions used are Neumann boundary conditions. For Upwind discretisations, Neumann boundary conditions and state constraints are the same.

The main difference between the LF discretisation and the Upwind scheme can be observed in the run times, see Table 1. The table contains run times for the LF discretisation using a fixed τ , manually optimised such that the method just remains stable. The iterative result using an Upwind discretisation has been achieved with a Gauss-Seidel-like scheme and an adaptive τ . Both iterations have been stopped at an equivalent rate of convergence, i.e. with a similar stopping criterion. The run times representatively reflect the time necessary to obtain a reasonable result with our implementation.

As we can observe, the run times of the scheme with an Upwind discretisation are significantly better than those for the LF discretisation. This fact, together with this scheme being much easier to implement and a clear stability bound for the time step size makes the Upwind discretisation clearly

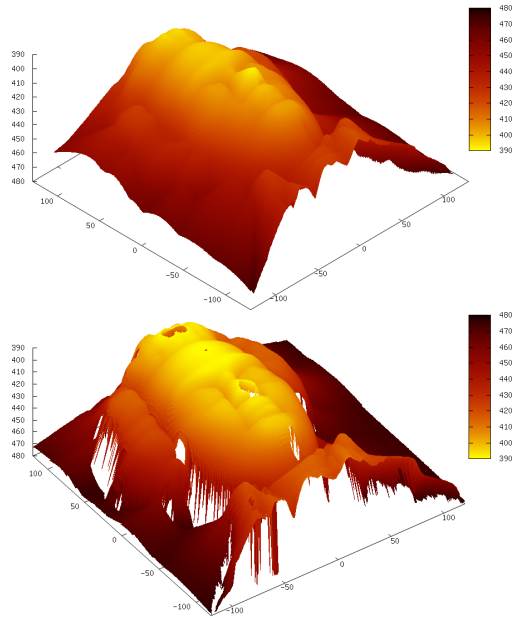


Fig. 2. Reconstructions. Top: Phong, Bottom: Oren-Nayar.

superior to the LF discretisation.

Finally, we also included run times for both experiments using a Fast Marching method implemented in the same way as proposed in [8]. Obviously, the run-times are even better. However, this method is more intricate to implement than the iterative Upwind solver, and it strongly depends on the right initialisation, which can be found for both models, but requires some non-trivial insight into the model. Since the Fast Marching method depends on the Upwind discretisation as well, it clearly shows the superiority of an Upwind discretisation compared to LF schemes.

5. CONCLUSION

We reviewed two advanced shape-from-shading models based on non-Lambertian reflectance. One was the Phong model, which extends a Lambertian reflectance model by specular highlights, the other the Oren-Nayar reflectance model, which replaces Lambertian reflectance by a more realistic model for rough surfaces.

We proposed to discretise the Hamilton-Jacobi equations with an Upwind discretisation, since they allow better performance to the commonly used Lax-Friedrichs schemes. In

Table 1. Run-times for the experiments (in seconds).

Model / Method	LF	Upwind	Fast Marching
Phong	79.8	13.5	0.87
Oren-Nayar	46.3	4.89	0.73

addition, they are much easier to implement. We derived upper bounds for the fictitious time step of both models, giving the reader a guide to implement these methods.

Experimentally, we verified the better performance of Upwind-based schemes and also tested an Upwind-based Fast Marching method on both reflectance models, which allowed for even better performance and qualitatively comparable results. Therefore, we advocate the use of Upwind-type schemes, even if it takes some effort on the theoretical side.

6. REFERENCES

- [1] E. Prados and Olivier Faugeras, “Shape from shading: A well-posed problem?,” in *Proc. 2005 IEEE Computer Society Conference on Computer Vision and Pattern Recognition*, San Diego, CA, June 2005, vol. 2, pp. 870–877, IEEE Computer Society Press.
- [2] M. Breuß, E. Cristiani, J.-D. Durou, M. Falcone, and O. Vogel, “Perspective shape from shading: Ambiguity analysis and numerical approximations,” Tech. Rep. 276, Department of Mathematics, Saarland University, Saarbrücken, Germany, September 2009.
- [3] O. Vogel, M. Breuß, and J. Weickert, “Perspective shape from shading with non-Lambertian reflectance,” in *Pattern Recognition*, G. Rigoll, Ed., vol. 5096 of *Lecture Notes in Computer Science*, pp. 517–526. Springer, Berlin, June 2008.
- [4] A. Ahmed and A. Farag, “Shape from shading under various imaging conditions,” in *CVPR*, 2007.
- [5] M. Crandall and P. L. Lions, “Two approximations of solutions of Hamilton-Jacobi equations,” *Mathematics of Computation*, vol. 43, no. 167, pp. 1–19, 1984.
- [6] E. Rouy and A. Tourin, “A viscosity solutions approach to shape-from-shading,” *SIAM Journal of Numerical Analysis*, vol. 29, no. 3, pp. 867–884, 1992.
- [7] O. Vogel, M. Breuß, and J. Weickert, “A direct numerical approach to perspective shape-from-shading,” in *Vision, Modeling, and Visualization*, H. Lensch et al., Ed., Saarbrücken, Germany, November 2007, pp. 91–100.
- [8] O. Vogel, M. Breuß, T. Leichtweis, and J. Weickert, “Fast shape from shading for Phong-type surfaces,” in *Scale Space and Variational Methods in Computer Vision*, X.-C. Tai et al., Ed., vol. 5567 of *Lecture Notes in Computer Science*, pp. 733–744. Springer, Berlin, 2009.
- [9] R. Zhang, P.-S. Tsai, J. Cryer, and M. Shah, “Shape from shading: A survey,” *IEEE Transactions on Pattern Analysis and Machine Intelligence*, vol. 21, no. 8, pp. 690–706, 1999.